J Nanostruct 14(3): 751-764, Summer 2024

RESEARCH PAPER

Tetrazole Derivatives from Quinaldic Acid: Estimation of the Biological and Antioxidant Properties

Enaam Fadil Mousa

Department of Chemistry, College of Science for Women University of Baghdad, Iraq

ARTICLE INFO

Article History:
Received 04 April 2024
Accepted 18 June 2024
Published 01 July 2024

Keywords:
Bacterial and Fungal Species
Biological and Antioxidant Properties
Molecular Docking
Quinaldic Acid Derivatives
Tetrazole Rings

ABSTRACT

This study focused on the synthesis of a variety of Schiff bases and their corresponding tetrazole derivatives. The Schiff bases were prepared by reacting quinaldic acid hydrazide with different aromatic aldehydes, followed by cyclization with sodium azide to form tetrazoles. The structures of the synthesized compounds were confirmed using spectroscopic techniques including FT-IR, XRD, FESEM, and ^{1}H and ^{13}C-NMR. Thin-layer chromatography (TLC) was utilized to verify the purity of the compounds. The biological properties of the synthesized compounds were investigated against two bacterial species (Staphylococcus epidermidis and Escherichia coli) and a fungal species (Candida albicans). Furthermore, blind molecular docking studies were performed to identify potential binding sites of these compounds within bacterial and fungal receptors. The antioxidant properties of several compounds were also examined, demonstrating antioxidant activity in some of the selected compounds. The results indicated that the synthesized tetrazole derivatives have significant biological and antioxidant activities, making them potential candidates for further pharmaceutical development.

How to cite this article
Mousa E. Tetrazole Derivatives from Quinaldic Acid: Estimation of the Biological and Antioxidant Properties. J Nanostruct, 2024; 14(3):751-764. DOI: 10.22052/JNS.2024.03.006

INTRODUCTION

Tetrazole derivatives are a versatile class of nitrogen, sulfur and halogen-containing heterocyclic compounds with a wide range of pharmacological applications [1-4]. The ability to modify the tetrazole ring by substitutions at five different positions such as 1, 2, 3, and 5 has led to discovery of compounds having diverse biological activities [5-8]. Pharmacologically active tetrazole compounds are well documented in the literature and several tetrazole-based drugs are currently available in the market [9, 10]. These tetrazole derivatives offer a promising avenue for drug discovery due to their structural diversity, biological properties [9, 11-13], remarkable pharmacokinetics, and adherence to Lipinski's rule of five [14, 15]. For these reasons, tetrazole-based compounds have become a popular scaffold in medicinal chemistry and drug discovery [16, 17], in various therapeutic areas such as anti-allergic [18], anti-inflammatory [19], antibiotic [20], antihypertensive [2], antitumor [11], antiviral [21] and receptor modulating properties [22].

The literature is replete with recent publications on tetrazole drugs, new synthesis methods, and new synthetic precursors. The discovery of tetrazoles by Swedish chemist Bladen in 1885 was a happy accident. Despite being a serendipitous finding, the field has marked the beginning of their exploration [23]. Tetrazoles have garnered

* *Corresponding Author Email: enaam.f@csw.uobaghdad.edu.iq*

sustained interest due to their versatility in coordination and medicinal chemistry. They serve as the diverse ligands in coordination chemistry offering a stable alternative to carboxylic acids in medicinal uses. Additionally, tetrazoles have been found to have various applications in materials science [24].

Keeping in view the above discussion, this study aimed at *(i)* synthesizing tetrazole derivatives derived from quinaldic acid, *(ii)* investigating the antimicrobial and antioxidant properties of the synthesized compounds and *(iii)* analysis of their potential interactions with receptors via molecular docking.

MATERIALS AND METHODS

Materials and instruments

For the determination of melting points of substances, UK's electrothermal melting point device was used while for monitoring reaction and assessing the purity of the synthesized products, thin-layer chromatography (TLC) was employed using aluminum plates coated in a coat of silica gel that is 0.25 mm thick. A mobile phase mixture of petroleum ether or hexane/ethyl acetate (in various ratios such as 2:1, 3:2, 1:1 v/v) was used. Using an iodine chamber, spots were observed. All chemicals used were from BDH Chemical Company and Merck. Fourier-transform infrared (FTIR) spectroscopy was performed using a SHIMADZU FT.IR-8400S infrared spectrometer located at Baghdad University, Iraq. Tetramethylsilane (TMS) was used as the internal standard for proton nuclear magnetic resonance (^{1}H-NMR) spectroscopic analysis conducted at 500 MHz. These NMR measurements were performed in the Chemistry Department of the University of Al-Basra. For XRD and FESEM, XRD-6000, Shimadzu, Japan and MIRA3, MIRA3, TESCAN, China (accelerating voltage = 25 kV) was used.

Synthesis of ethyl Quinaldate (1)

For the synthesis of ethyl Quinaldate 1, a mixture of 30 mL pure ethanol, 5 g (0.06 mol) quinaldic acid, and a few drops concentrated sulfuric acid was refluxed for 12 hours with continuous reaction monitoring by TLC. After completion, the reaction mixture was cooled with crushed ice, followed by neutralization with sodium bicarbonate, and finally extraction was done with dichloromethane. This resulted in the formation of brown gummy precipitate with 82% yield. FT-IR analysis (KBr) confirmed the presence of a carbonyl group (1721 cm^{-1}) and a carbon-oxygen bond (1216 cm^{-1}) highlighting the successful synthesis of ethyl Quinaldate 1.

Synthesis of Quinaldic acid hydrazide 2

A solution of 4 grams of compound (1) in 20 mL of pure ethanol was treated with an excess of hydrazine hydrate with continuous reaction monitoring by TLC during a 5-hour reflux period. After completion, the solvent and unreacted hydrazine were removed under reduced pressure. The resulting precipitate was then recrystallized from 70% ethanol that resulted in yielding 73% of yellow crystals. FT-IR analysis (KBr) confirmed the presence of NH_2 (3431 and 3294 cm^{-1}), N-H (3294 cm^{-1}), and C=O (1652 cm^{-1}) functional groups highlighting the successful synthesis of Quinaldic acid hydrazide 2.

Standard protocol for synthesis of Schiff base and its derived compounds

Synthesis of Schiff base (Sch1-Sch6)

A series of Schiff bases were synthesized by reacting compound (2) (0.5 g, 0.0026 mol) with equimolar amounts of different aldehydes in a mixture of 20 mL pure ethanol and 3-5 drops of glacial acetic acid. The reaction mixture was refluxed for nearly six hours, followed by cooling and filtering the resulting precipitate which were the washed with methanol, and recrystallized [25]. The details of these compounds are as below:

N'-(4-bromobenzylidene) quinoline-2-carbohydrazide (Sch1)

Yellow precipitate, with M.P. of 118-120 °C, yield: 75%, M. F: $C_{17}H_{12}BrN_3O$, M. wt: 354.21 g/ mole, FT-IR (KBr); The measurements are 3245 cm^{-1} corresponding to vibration of N-H bond, 1641 cm^{-1} (overlapping) with the stretching vibrations of carbonyl group, 1625 cm^{-1} representing stretching vibrations for imine group, and 553 cm^{-1} referring to stretching vibration for (C-Br) bond.

N'-(4-chlorobenzylidene) quinoline-2-carbohydrazide (Sch2)

Yellow precipitate, with M.P. 108-110 °C, yield: 69%, M. F.: $C_{17}H_{12}ClN_3O$, M. wt: 309.75 g/ mole, FT-IR (KBr); 3247 cm^{-1} referring to υ(N-H), 1645cm^{-1} (overlapping) correspond to stretching vibrations of carbonyl group and 1623 cm^{-1} referring to stretching vibrations for imine group.

N'-(4-(dimethyl amino) benzylidene) quinoline-2-carbohydrazide (Sch3)

Pell yellow precipitate, with M.P. (110-112) °C, yield of 79%, M. F.: $C_{19}H_{18}N_4O$, M. wt: 318.38 g/ mole, FT-IR (KBr); 3292 cm^{-1} referring to υ(N-H), 1645cm^{-1} (overlapping) represents stretching vibrations of carbonyl group, 1600 cm^{-1} refers to stretching vibrations for imine group.

N'-(4-nitrobenzylidene) quinoline-2-carbohydrazide (Sch4)

Yellow precipitate, with M.P. (122-124) °C, yield of 82%, M. F.: $C_{17}H_{12}N_4O_3$, M. wt: 320.31 g/ mole, FT-IR (KBr); 3166 cm^{-1} represents stretching vibrations for N-H bond, 1670cm^{-1} refers to the stretching vibrations of carbonyl group, 1596 cm^{-1} corresponds to the stretching vibrations for imine group while band at 1521 cm^{-1} and 1344 cm^{-1} refers to NO_2 group.

N'-benzylidenequinoline-2-carbohydrazide (Sch5)

Yellow precipitate, M.P. (154-156) °C, yield: 81%, M.F.: $C_{17}H_{13}N_3O$, M. wt: 275.31 g/ mole, FT-IR (KBr); 3244 cm^{-1} represents stretching vibrations for N-H bond, 1712 cm^{-1} represents stretching vibrations of carbonyl group while 1623 cm^{-1} represents stretching vibrations for imine group.

N'-(4-hydroxybenzylidene) quinoline-2-carbohydrazide (Sch6)

Yellow precipitate, M.P. (154-156) °C, yield: 60%, M.F.: $C_{17}H_{13}N_3O_2$, M. wt: 291.31 g/ mole, FT-IR (KBr); 3303 cm^{-1} [υ(O-H)], 3249 cm^{-1} [υ(N-H)], 1649cm^{-1} [υ(C=O)], 1623 cm^{-1} [υ(C=N)].

Synthesis of tetrazoles (T1-T6)

For the synthesis of tetrazoles (T1-T6), 0.11 moles of Schiff bases were dissolved in 10 mL of THF and reacted with an equivalent amount of sodium azide. This reaction mixture was refluxed for nearly 12 hours, with progress monitored continuously by TLC. Upon completion, the mixture was poured onto crushed ice followed by the filtration of the resulted precipitate and recrystallization from petroleum ether. The details of these compounds are as below:

(5-(4-bromophenyl)-1H-tetrazol-1-yl) quinoline-2-carboxamide (T1)

White precipitate, M.P. (204-206) °C, yield: 63%, M.F.: $C_{17}H_{11}BrN_6O$, M. wt: 395.22 g/ mole, FT-IR (KBr); 1269 cm^{-1} (N-N=N-), 1120 and 1180 cm^{-1} (Tetrazole ring), [υ(N-H)] 3388 cm^{-1}, [υ(C=O)]1720 cm^{-1} , [υ(N=N)]1403 cm^{-1} and 522 cm-1 [υ(C-Br)]. Further, ^{1}H NMR: δ 8.25 ppm (1H, s, NH), δ 6.68-7.8.59 (10 H, m, Ar-H) and ^{13}C NMR: δ 160 ppm (1C, C=O), δ 152 (1C, tetrazole C=N), 112-149 (10 C, Ar Carbone).

(5-(4-chlorophenyl)-1H-tetrazol-1-yl) quinoline-2-carboxamide (T2)

White precipitate, M.P. (224-226) °C, yield: 63%, M.F.: $C_{17}H_{11}ClN_6O$, M. wt: 350.77 g/ mole, FT-IR (KBr); 1274 cm^{-1} (N-N=N-), 1108 and 1182 cm^{-1} (Tetrazole ring), [υ(N-H)] 3429 cm^{-1}, [υ(C=O)] 1714cm^{-1}, [υ(N=N)] 1413 cm^{-1} and 844cm^{-1} [υ(C-Cl)]. Further, ^{1}H NMR: 8.87 ppm (1H,s,-NH), 7.76-7.55 (10 H, m, Ar-H) and ^{13}C NMR: ^{13}C NMR: δ 166 ppm (1C, C=O), δ 149 (1C, tetrazole C=N), 121-147 (10 C, Ar Carbone).

(5-(4-(dimethylamino)phenyl)-1H-tetrazol-1-yl) quinoline-2-carboxamide (T3)

White precipitate, M.P. (192-194) °C, yield: 63%, M.F.: $C_{19}H_{17}N_7O$, M. wt: 359.39 g/ mole, FT-IR (KBr); 1285 cm^{-1} (N-N=N-), 1108 and 1138 cm^{-1} (Tetrazole ring), 3423 cm^{-1} [υ(N-H)], 1712 cm^{-1} [υ(C=O)], 1402 cm^{-1} [υ(N=N)], 2945 cm^{-1} [υ(C-H) aliph.].

(5-(4-nitrophenyl)-1H-tetrazol-1-yl)quinoline-2-carboxamide (T4)

White precipitate, M.P. (254-256) °C, yield: 63%, M.F.: $C_{17}H_{11}N_7O_3$, M. wt: 361.32 g/ mole, FT-IR (KBr); 1288 cm^{-1} (N-N=N-), 1108 with 1164 cm^{-1} (Tetrazole ring), 3456 cm^{-1} [υ(N-H)], 1633 cm^{-1} [υ(C=O)], 1400 cm^{-1} [υ(N=N)], 1521 and 1344 cm^{-1} [υ(NO2)]. Further, ^{1}H NMR: δ 8.15 ppm (1H, s, NH), δ 3.38 ppm (6H, s, CH_3N), δ 7.34 -7.8.71 ppm (10 H, m, Ar-H) and ^{13}C NMR: δ 165 ppm (1C, C=O), δ 152 (1C, tetrazole C=N), δ 40.52 ppm (2C, C=O),129-140 (10 C, Ar Carbone).

(5-phenyl-1H-tetrazol-1-yl)quinoline-2-carboxamide (T5)

yellow precipitate, M.P. (120-122) °C, yield: 63%, M.F.: $C_{17}H_{12}N_6O$, M. wt: 316.32 g/ mole, FT-IR (KBr); 1234 cm^{-1} (N-N=N-), 1120 with 1151 cm^{-1} (Tetrazole ring), 3456 cm^{-1} [υ(N-H)], 1633 cm^{-1} [υ(C=O)], 1400 cm^{-1} [υ(N=N)].

(5-(4-hydroxyphenyl)-1H-tetrazol-1-yl)quinoline-2-carboxamide (T6)

White precipitate, M.P. (254-256) °C, yield:

63%, M.F.: $C_{17}H_{12}N_6O_2$, M. wt: 332.32 g/mole, FT-IR (KBr); 1284 cm^{-1} (N-N=N-), 1091 cm^{-1} with 1172 cm^{-1} (Tetrazole ring), 3676 cm^{-1} [υ(O-H)], 3456 cm^{-1} [υ(N-H)], 1700 cm^{-1} over lapping [υ(C=O)] and 1396 cm^{-1} [υ(N=N)].

Biological activity

The antibacterial activity of numerous Schiff bases as well as their tetrazole derivatives was investigated using the agar diffusion technique utilizing cap plates and incubation at 37 ℃ for 24 hours. The inhibition zone was estimated in micrometers.

Activity of radical scavenging in DPPH (1,1-Diphenyl-2-picryl-hydrazyl)

For DPPH activity, 100 milliliters of methanol were used to dissolve 4 milligrams of DPPH, and aluminum foil was placed over the test tubes to keep the solution opaque. Several concentrations (100, 50, 25, 12.5, and 6.25 ppm) of [T1, T4-T6] were prepared. A 100 ppm stock solution was initially prepared by dissolving 1 mg of the compound in 10 mL of methanol. Subsequent dilutions were made to obtain the lower concentrations as per requirement. Vitamin C (ascorbic acid) was prepared in equivalent quantities to the selected manufactured compounds (T1, T4-T6). The antioxidant activity of these compounds and vitamin C was investigated by using the DPPH free radical scavenging method. One milliliter of each diluted or standard solution (6.25, 12.5, 25, 50, and 100 ppm) was added to 1 mL of DPPH solution. After incubation for one hour at 37°C, the absorbance of each solution was measured at 517 nm using a spectrophotometer. All measurements were performed in triplicate (n=3). To calculate the potential to scavenge DPPH radicals, the following formula was utilized:

$$I\% = \frac{Abs_{sample} - Abs_{blank}}{Abs_{blank}} \text{ x } 100 \quad (1)$$

A few of the recently produced derivatives shown strong scavenging percentages and antioxidant activity against the DPPH free radical. Thus, as indicated in Table 2 below, the compounds that provided antioxidant were chosen, additional testing was carried out, and the IC50 value was retrieved.

Molecular docking study

ChemDraw Professional 15.0 was used to create structural representations of the compounds [26]. The formula with the lowest energy, or the formula to minimize energy, was then chosen using the chem3D tool, and it was stored in PDB format [27]. A protein was selected from the Protein Data Bank and also saved in PDB format [28]. Next, using the Autodock Tool program, the protein and compound were formed, polar hydrogens and charges were added, and PDBQT format was utilized for storage. [29]. Using Autodock Vina and the PyRx program, the chemical and protein underwent blind molecular docking simulation. The optimal conformation was chosen and stored in the PDB extension. [30]. Furthermore, Discovery Studio 2024 Client was used for visualization of the 2D and 3D molecular interactions [31].

RESULTS AND DISCUSSION

Chemistry of tetrazole synthesis from Quinaldic acid

Quinaldic acid was initially esterified using the Fischer esterification method. The resulting ester was then converted to a hydrazide by its reaction with hydrazine hydrate. Subsequent treatment of the hydrazide with various aldehydes resulted in the synthesis of the Schiff bases. These Schiff bases underwent cyclization to tetrazole rings upon reaction with sodium azide (Fig. 1a). The progress of each step was monitored using TLC, infrared (IR), and NMR spectroscopy. The changes in the expansion readings of the prepared compounds were observed. The value of the carbonyl spectral band in the acid was changed from 1701 cm^{-1} to 1721 cm^{-1} of the ester with a complete disappearance of the band of the acidic hydroxyl and the appearance for C-O peak of the ester at 1216 cm^{-1}. The hydrazide exhibited a shift in carbonyl peak from the ester region (1721 cm^{-1}) to the amide region (1652 cm^{-1}), along with the disappearance of NH_2 and NH peaks and the appearance of new peaks linked with NH_2 (3431 cm^{-1}) and NH (3294 cm^{-1}) stretching vibrations. In the Schiff bases, the NH_2 peak disappeared with the formation of a new C=N peak in the range of 1600-1645 cm^{-1}. The tetrazole compounds revealed the disappearance of distinctive Schiff base peak and appearance of new peaks linked with tetrazole ring: N-N=N stretching at 1234-1288 cm^{-1} and tetrazole ring vibrations at 1091-1120 cm^{-1} and 1138-1182 cm^{-1}. Furthermore, NMR

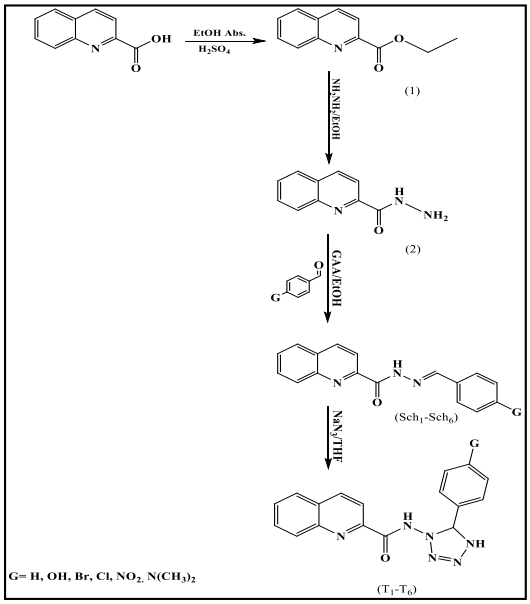

(a)

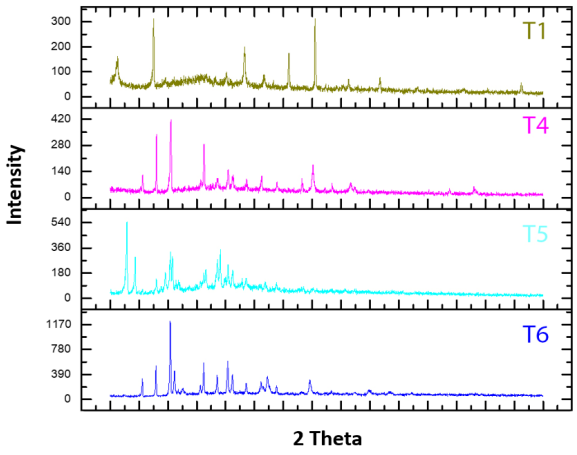

(b)

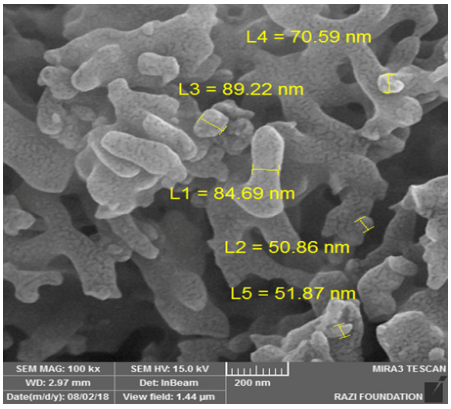

(c)

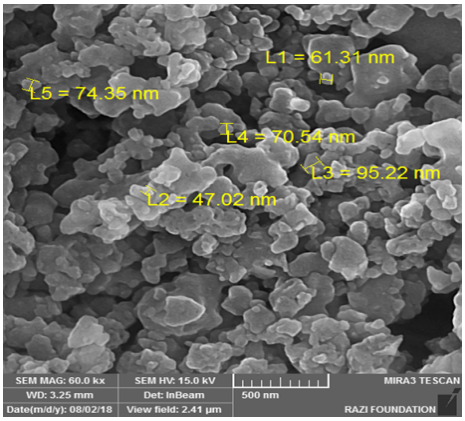

(d)

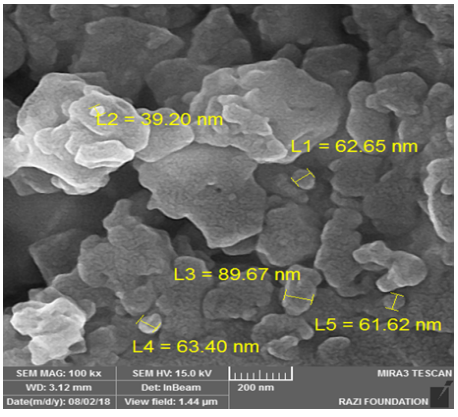

(e)

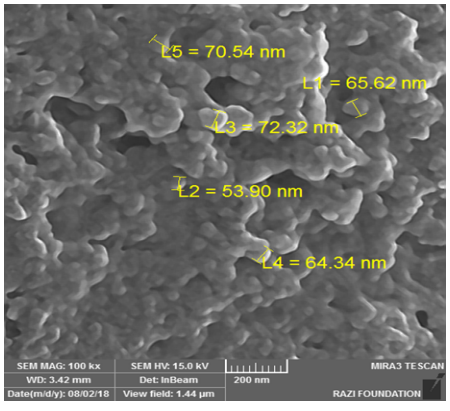

(f)

Fig. 1. (a) Scheme of all steps of tetrazole synthesis from Quinaldic acid, (b) XRD analysis of T1, T4, T5, T6, FESEM analysis of (c) T1, (d) T4, (e) T5 and (f) T6.

analysis of selected tetrazole compounds (T1, T2, and T4) confirmed the presence of distinctive signals characteristic of tetrazole ring, as detailed in sub-section 2.5. Based on the combined IR

Table 1. Summary of the biological activity of synthesized compounds.

Compund No.	Bactericidal action		Antifungal activity
	Staphylococcus epidermidis	*E. coli*	*Candida albicans*
Sch1	24	17	15
Sch3	17	12	17
Sch5	11	9	21
Sch6	14	10	21
T1	12	15	24
T3	-ev	10	16
T5	12	15	14
T6	10	10	15
Metronidizole	-ev	-ev	12
Ampiciline	12	12	-ev
DMSO	-ev	-ev	-ev

(-ev) = No inhibition

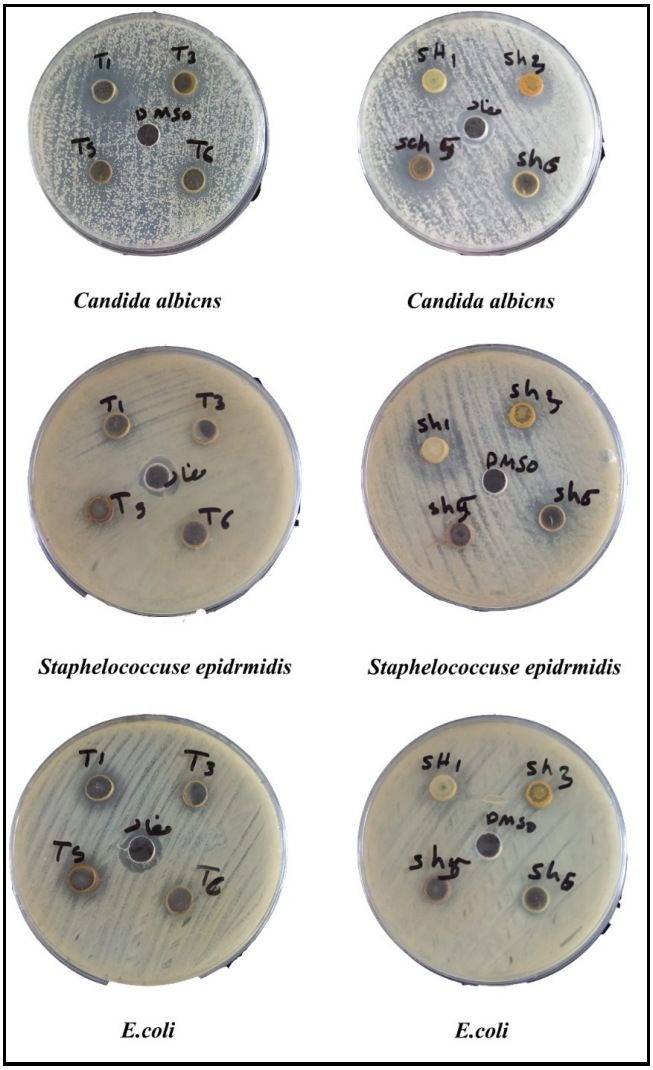

Fig. 2. Inhibition zone of the selected compounds.

and NMR spectral evidence, successful synthesis of target tetrazole compounds was confirmed. Additionally, the XRD (Fig. 1b) and FESEM analysis (Fig. 1c-f) of T1, T4, T5 and T6 revealed that the prepared compounds are of nano-size i.e., nanomaterials. These results further confirmed the successful synthesis of each nanomaterial that exhibits the sharp peaks in XRD revealing the crystallinity present in them. Furthermore, the porosity and particle size of each material can be obvious in FESEM images.

Biological activity

Results revealed that the effectiveness against Gram-positive bacteria was demonstrated by compounds Sch3 and Sch5, but good action against microorganisms that are gram-negative was demonstrated by deivatives T1 with T5. The

Table 2. Antioxidant activity as stated by Phongpaichit (2007).

IC50 (µg/mL	Mark
10-50 µg/mL	Strong Antioxidant Activity
50-100 µg/mL	Intermediate Antioxidant Activity
>100 µg/mL	Weak Antioxidant Activity

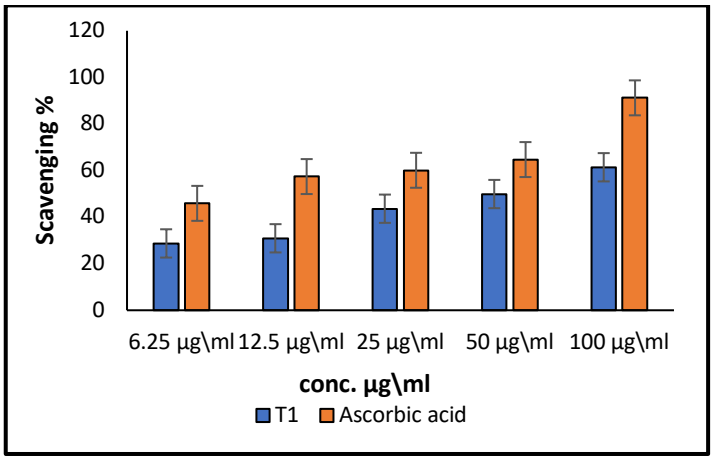

Fig. 3. Scavenging percentage for compound T1.

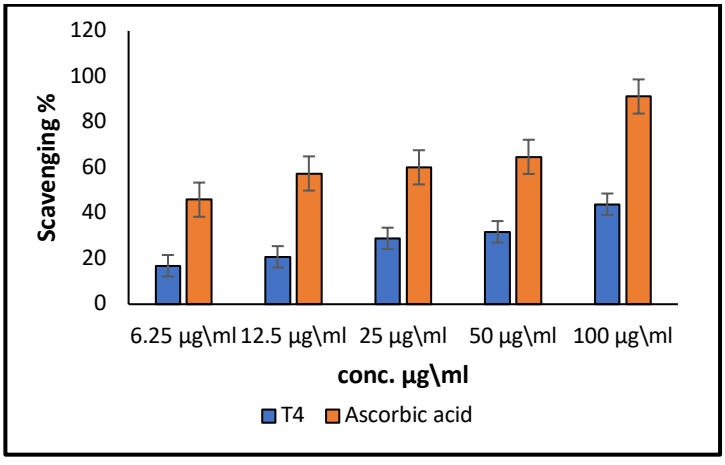

Fig. 4. Scavenging percentage for compound T4.

compound T3 gave less activity against both types when compared with ampicillin as a standard substance. Results of the study are summarized in Table 1 and Fig. 2. Further, it was observed that the prepared and selected compounds for measurement gave good activity against fungi, as the compounds T1 and Sch5 gave the best activity against *Candida albicans* when compared with

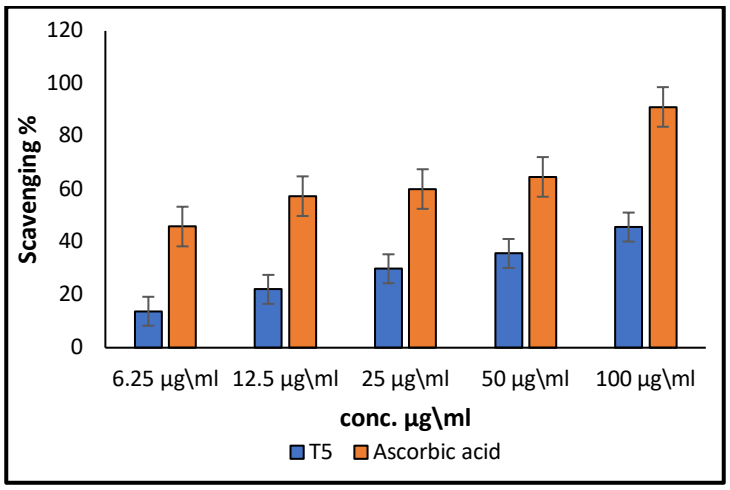

Fig. 5. Scavenging percentage for compound T5.

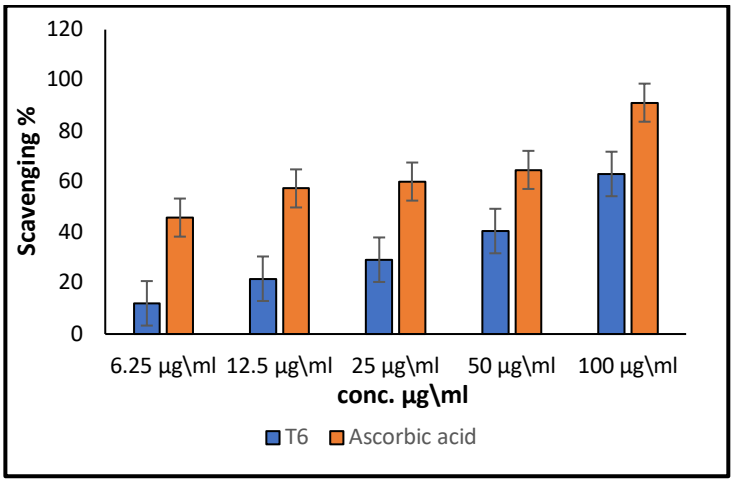

Fig. 6. Scavenging percentage for compound T6.

Table 3. Antioxidant properties of particular compounds.

Comp. No.	Scavenging %					Linear eq.	R^2	Ic50
	6.25 µg\ml	12.5 µg\ml	25 µg\ml	50 µg\ml	100 µg\ml			
T1	28.7	30.9	43.6	49.9	61.4	y = 0.3404x + 29.708	R^2 = 0.9135	59.61
T4	16.9	20.8	28.9	31.8	43.9	y = 0.2674x + 18.1	R^2 = 0.9399	119.29
T5	13.8	22.1	29.9	35.7	45.7	y = 0.303x + 17.7	R^2 = 0.8859	106.6
T6	12.1	21.8	29.3	40.6	63.1	y = 0.5081x + 13.692	R^2 = 0.975	71.45
Ascorbic acid	45.9	57.4	60.1	64.7	91.2	y = 0.4282x + 47.267	R^2 = 0.946	6.38

Metronidizole as a standard substance.

DPPH radical scavenging activity

Study revealed that several of the newly synthesized compounds exhibited significant free radical scavenging activity against DPPH (Fig. 3 to 6). Based on these promising results, we selected compounds demonstrating antioxidant properties for further investigation. Accordingly, inhibitory concentrations (IC_{50}) values were recorded and

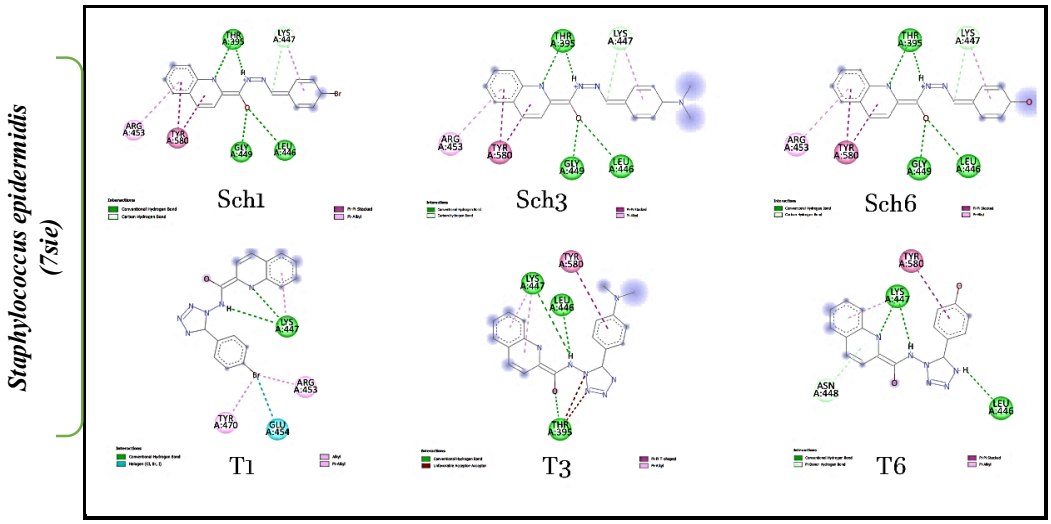

Fig. 7. 2D interaction selected compounds and *Staphylococcus epidermidis resaptor (7sie).*

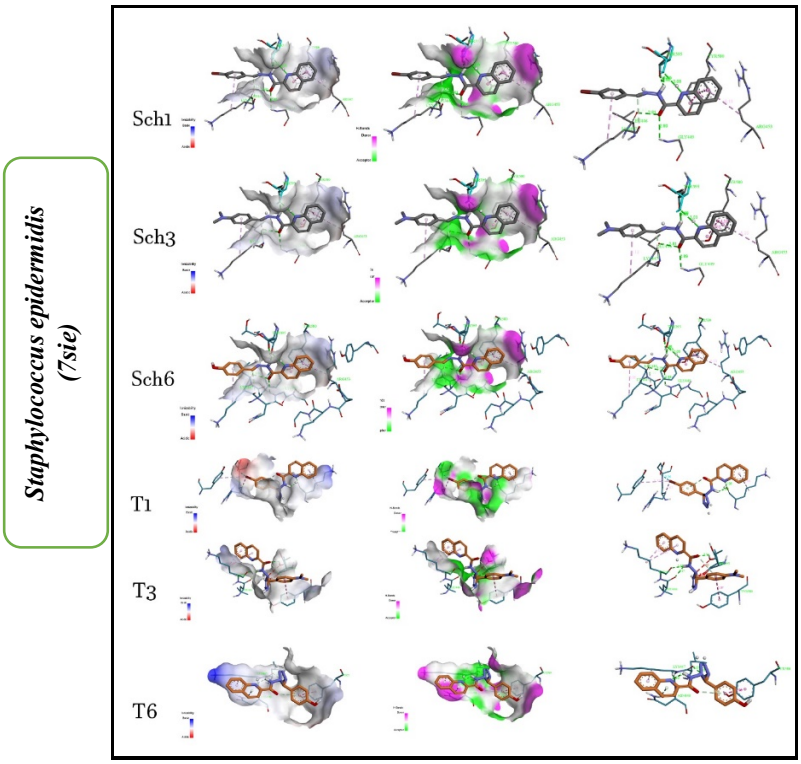

Fig. 8. 3D interaction selected compounds and *Staphylococcus epidermidis resaptor (7sie).*

summarized in Table 2. Herein, we applied the antioxidant activity classification which depends on IC_{50} range values that published by Phongpaichit, as summarized in Table 2.

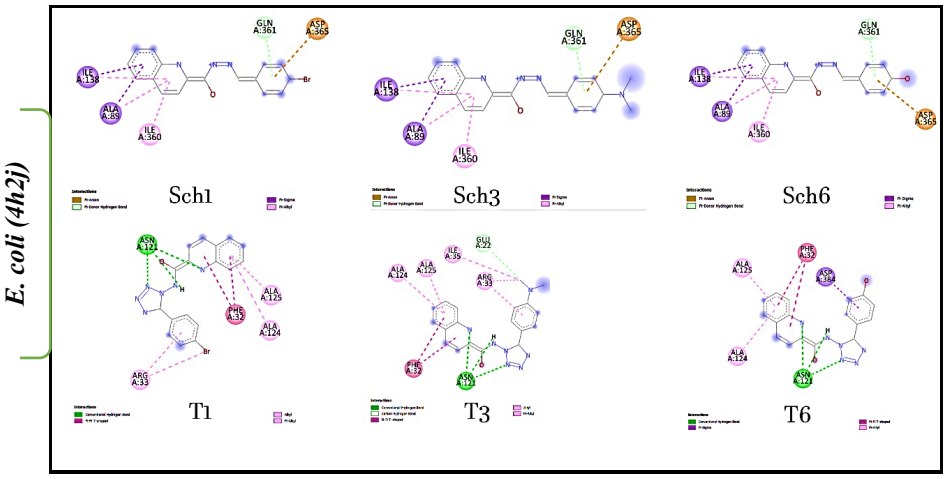

Fig. 9. 2D interaction selected compounds and *Candida albicans resaptor E. coli (4h2j).*

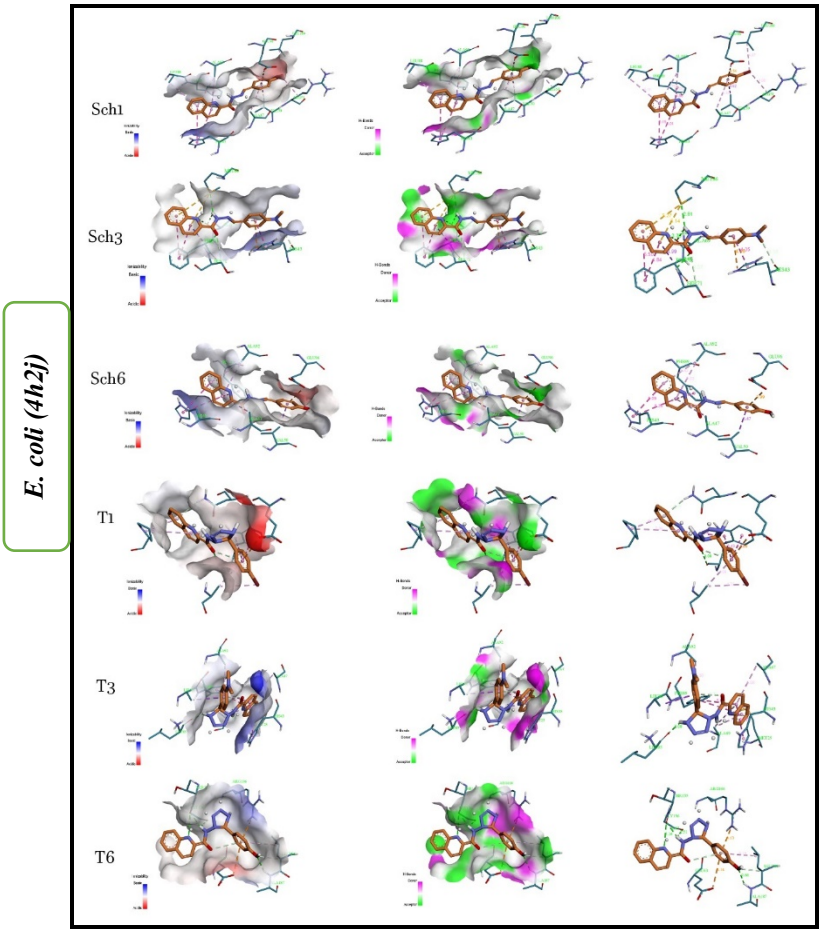

Fig. 10. 2D interaction selected compounds and *Candida albicans resaptor E. coli (4h2j).*

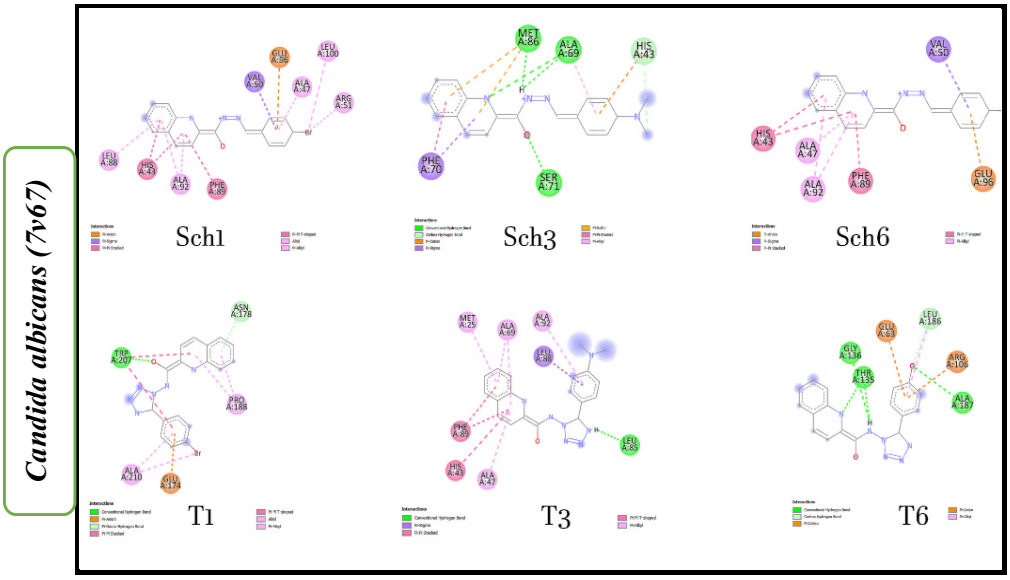

Fig. 11. 2D interaction selected compounds and *Candida*

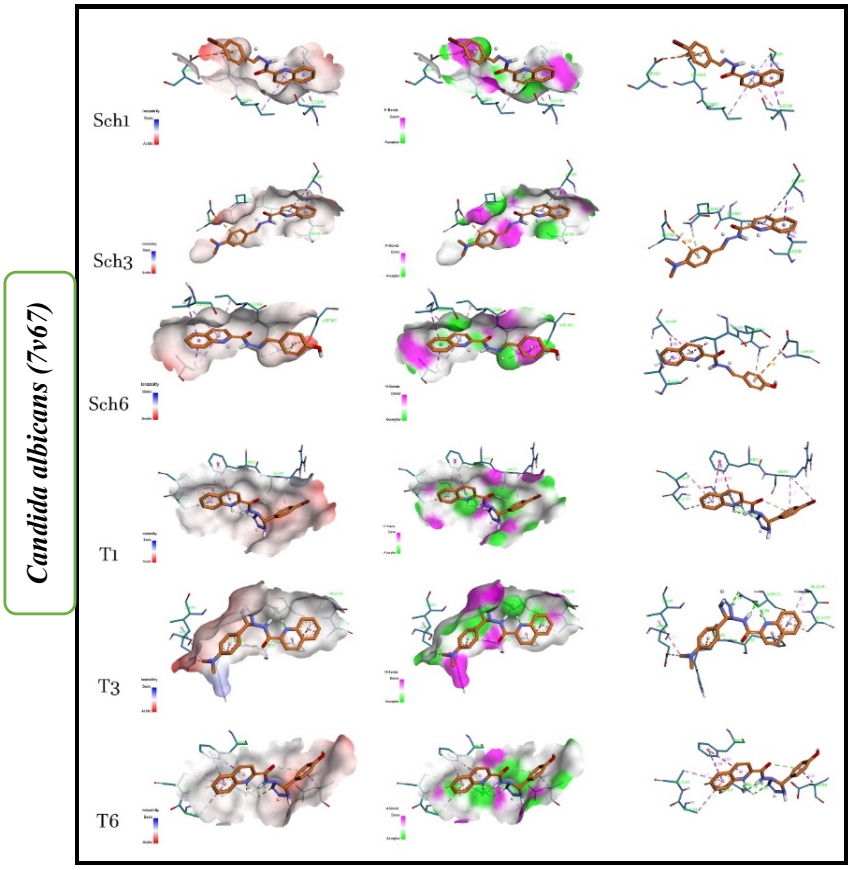

Fig. 12. 3D interaction selected compounds and *Candida albicans resaptor (7v67).*

a. Every chosen compound shown powerful antioxidative properties as tabulated in Table 3.

b. The highest anti-oxidant activity and the lowest IC_{50} values were found for compound (T1)

c. Derivatives (T1) with (T6) possess intermediate antioxidant activity.

Table 4. Binding energies for selected compounds.

Comp. No.	Binding enrgy Kcal/mol		
	Staphylococcus epidermidis (7sie)	*E. coli (4h2j)*	*Candida albicans (7v67)*
Sch1	-9.4	-9.6	-8.3
Sch3	-9.7	-9	-8.5
Sch6	-9.5	-9	-8.2
T1	-9.7	-9.1	-9.6
T3	-8.4	-8.7	-10
T6	-8.6	-8.9	-9.8

Table 5. Active sides dimensions on receptors for selected compounds.

Comp. No.	Active side								
	Staphylococcus epidermidis (7sie)			*E. coli (4h2j)*			*Candida albicans (7v67)*		
	X	Y	Z	X	Y	Z	X	Y	Z
Sch1	15.47	17.76	35.36	44.09	35.37	59.27	-7.48	-44.40	-3.96
Sch3	15.40	18.37	35.05	40.93	41.53	53.48	-6.99	-44.68	-3.77
Sch6	15.45	18.11	35.18	43.89	34.55	59.36	-7.26	-44.51	-3.89
T1	13.47	17.16	34.09	30.87	26.50	34.26	-30.24	-43.33	-3.18
T3	14.36	17.77	34.67	44.48	39.91	58.91	-30.62	-43.23	-2.89
T6	13.67	15.92	33.85	39.28	15.70	48.76	-30.42	-43.62	-2.86

Table 6. Interactions, residues and distances for selected compounds and receptors.

Com. No.	*Staphylococcus epidermidis (7sie)*			*E. coli (4h2j)*			*Candida albicans (7v67)*		
Sch1	Residue	Interaction	Distance A°	Residue	Interaction	Distance A°	Residue	Interaction	Distance A°
	THR A:395	Conventional H. B.	1.59	GLU A:96	Pi- anion	4.52	ASP A:365	Pi-anion	4.92
	THR A:395	Conventional H. B.	3.08	VAL A:50	Pi- sigma	3.52	GLN A:361	Pi- donor H.B.	2.94
	GLY A:449	Conventional H. B.	2.90	PHE A:89	Pi-pi stacked	4.86	ALA A:89	Pi- sigma	3.98
	LEU A:446	Conventional H. B.	2.81	HIS A:43	Pi-pi T-shape	5.01	ILE A:138	Pi- sigma	3.90
	LYS A:447	Carbon H.B.	3.42	HIS A:43	Pi-pi T-shape	5.19	ALA A:89	Pi- alkyl	4.91
	TYR A:580	Pi-pi stacked	3.83	LEU A:100	Alkyl	4.67	ILE A:138	Pi- alkyl	5.12
	TYR A:580	Pi-pi stacked	4.01	ARG A:51	Alkyl	4.06	ILE A:360	Pi- alkyl	4.75
	ARG A:453	Pi-alkyl	5.13	ALA A:47	Pi- alkyl	5.30			
	LYS A:447	Pi-alkyl	5.16	ALA A:92	Pi- alkyl	4.77			
				ALA A:92	Pi- alkyl	5.00			
				LEU A:88	Pi- alkyl	5.11			
Sch3	Residue	Interaction	Distance A°	Residue	Interaction	Distance A°	Residue	Interaction	Distance A°
	THR A:395	Conventional H. B.	1.59	ALA A:69	Conventional H.B.	3.03	ASP A:365	Pi-anion	4.98
	THR A:395	Conventional H. B.	3.03	ALA A:69	Conventional H.B.	3.30	GLN A:361	Pi- donor H.B.	2.98
	GLY A:449	Conventional H. B.	2.89	SER A:71	Conventional H.B.	2.45	ALA A:89	Pi- sigma	3.97
	LEU A:446	Conventional H. B.	2.81	MET A:86	Conventional H.B.	2.81	ILE A:138	Pi- sigma	3.89
	LYS A:447	Carbon H.B.	3.43	HIT A:43	Carbon H.B.	3.18	ALA A:89	Pi- alkyl	4.86
	TYR A:580	Pi-pi stacked	3.83	MET A:86	Pi- cation	5.14	ILE A:138	Pi- alkyl	5.09
	TYR A:580	Pi-pi stacked	4.00	MET A:86	Pi- sulfur	5.27	ILE A:360	Pi- alkyl	4.78
	ARG A:453	Pi-alkyl	5.20	PHE A:70	pi- sigma	3.99			
	LYS A:447	Pi-alkyl	5.13	PHE A:70	Pi-pi stacked	4.84			
				PHE A:70	Pi-pi stacked	4.55			
				ALA A:69	Pi-alkyl	4.69			
Sch6	Residue	Interaction	Distance A°	Residue	Interaction	Distance A°	Residue	Interaction	Distance A°
	THR A:395	Conventional H. B.	1.59	GLU A:96	Pi- anion	3.99	ASP A:365	Pi-anion	5.00
	THR A:395	Conventional H. B.	3.00	VAL A:50	Pi- sigma	3.47	GLN A:361	Pi- donor H.B.	3.01
	GLY A:449	Conventional H. B.	2.88	HIS A:43	Pi-pi stacked	5.09	ALA A:89	Pi- sigma	3.96
	LEU A:446	Conventional H. B.	2.91	HIS A:43	Pi-pi stacked	5.25	ILE A:138	Pi- sigma	3.90
	LYS A:447	Carbon H.B.	3.39	PHE A:89	Pi-pi T- shaped	4.81	ALA A:89	Pi- alkyl	4.87
	TYR A:580	Pi-pi stacked	3.80	ALA A:47	Pi- alkyl	5.23	ILE A:138	Pi- alkyl	5.10

	TYR A:580	Pi-pi stacked	3.97
	ARG A:453	Pi-alkyl	5.06
	LYS A:447	Pi-alkyl	5.23
	ALA A:92	Pi- alkyl	4.62
	ALA A:92	Pi- alkyl	5.03
	ILE A:360	Pi- alkyl	4.77

	Residue	Interaction	Distance A°
T1	LYS A:447	Conventional H. B.	2.69
	LYS A:447	Conventional H. B.	2.98
	GLU A:3454	Halogen	3.34
	ARG A: 453	Alkyl	4.07
	TYR A:470	alkyl	5.17
	LYS A:447	Pi-alkyl	4.99
	TRP A:207	Conventional H.B.	3.8
	GLU A:174	Pi- anion	3.69
	ASN A:178	pi- donor H.B.	3.80
	TRP A:207	Pi- pi stacked	4.92
	TRP A:207	Pi- pi stacked	5.43
	TRP A:207	Pi- pi T-shaped	5.48
	PRO A:188	Alkyl	5.09
	ALA A:210	Alkyl	4.32
	PRO A:188	Pi- alkyl	4.01
	ALA A:210	Pi- alkyl	4.06
	ASN A:121	Conventional H.B.	2.21
	ASN A:121	Conventional H.B.	2.62
	ASN A:121	Conventional H.B.	2.97
	PHE A:32	Pi-pi T-shaped	5.13
	PHE A:32	Pi-pi T-shaped	5.22
	ARG A:33	alkyl	4.66
	ARG A:33	Pi- alkyl	4.77
	ALA A:124	Pi- alkyl	5.23
	ALA A:125	Pi- alkyl	4.64

	Residue	Interaction	Distance A°
T3	THR A395	Conventional H. B.	2.31
	LEU A:446	Conventional H. B.	2.31
	LYS A:447	Conventional H. B.	2.97
	TYR A:580	Pi-pi stacked	5.07
	LYS A:447	Pi-alkyl	4.35
	LYS A:447	Pi-alkyl	5.06
	THR A:395	Unfavorable acceptor accepter	2.80
	THR A:395	Unfavorable acceptor accepter	2.92
	LEU A:85	Conventional H.B.	2.08
	LEU A:88	Pi- sigma	3.93
	HIS A:43	Pi-pi stacked	5.13
	PHE A:89	Pi-pi T-shaped	3.30
	PHE A:89	Pi-pi T-shaped	5.01
	MET A:25	Pi- alkyl	4.75
	ALA A:47	Pi- alkyl	5.08
	ALA A:69	Pi- alkyl	4.07
	ALA A:69	Pi- alkyl	5.33
	ALA A:92	Pi- alkyl	5.00
	ASN A:121	Conventional H.B.	2.21
	ASN A:121	Conventional H.B.	2.74
	ASN A:121	Conventional H.B.	2.89
	GLU A:22	Carbon H.B.	3.54
	PHE A:32	Pi-pi T-shaped	5.24
	PHE A:32	Pi-pi T-shaped	5.26
	ARG A:33	alkyl	4.53
	ILE A:35	alkyl	5.02
	ARG A:33	Pi- alkyl	4.93
	ALA A:124	Pi- alkyl	4.91
	ALA A:125	Pi- alkyl	4.60

	Residue	Interaction	Distance A°
T6	LEU A:446	Conventional H. B.	2.17
	LYS A:447	Conventional H. B.	2.93
	LYS A:447	Conventional H. B.	2.41
	ASN A:448	Pi-donor H.B.	3.17
	TYR A:580	Pi-pi stacked	3.83
	LYS A:447	Pi-alkyl	5.36
	THR A:135	Conventional H.B.	2.13
	THR A:135	Conventional H.B.	2.51
	GLY A:136	Conventional H.B.	3.14
	ALA A:187	Conventional H.B.	2.66
	LEU A:186	Carbon H.B.	3.34
	GLU A:63	Pi-cation	4.14
	ARG A:106	Pi- anion	3.63
	LEU A:186	Pi- alkyl	5.19
	ASN A:121	Conventional H.B.	2.18
	ASN A:121	Conventional H.B.	2.62
	ASN A:121	Conventional H.B.	2.99
	ASP A:384	Pi-sigma	3.97
	PHE A:38	Pi-pi T-shaped	5.09
	PHE A:38	Pi-pi T-shaped	5.52
	ALA A:124	Pi- alkyl	5.26
	ALA A:125	Pi- alkyl	4.64

d. Compounds (T4) and (T5) week antioxidant activity.

Molecular docking

The energy of binding between the chemicals and the protein is displayed in Table 4. The relationships between the compounds and the protein residues at the active site, as well as the kinds of interactions and the strength of the link between the residues and the compound, are displayed in Tables 5 and 6 and Fig. 7 to 12.

CONCLUSION

A series of novel Schiff bases and their corresponding tetrazolic derivatives were synthesized. The Schiff bases were prepared by reacting a hydrazide derived from quinaldic acid with different aromatic aldehydes. Subsequent reaction with sodium azide yielded the desired tetrazolic compounds. The structures of the synthesized compounds were confirmed by different spectral analysis including FT-IR, XRD, FESEM, ^{1}H, ^{13}C-NMR and their purity was verified using thin-layer chromatography (TLC). The biological activities of selected compounds were evaluated against *Escherichia coli, Staphylococcus* bacteria, and *Candida* fungi. Results revealed that the compound S1 exhibited significant antibacterial activity against both *Escherichia coli and Staphylococcus* bacteria. Derivatives S3 and S6 demonstrated notable activity against *Staphylococcus*, while compounds T1 and T5 were highly effective against *E. coli.* All compounds exhibited antifungal activity against *Candida* fungi, with T1, S5, and S6 displaying strong inhibitory effects. All results were compared with ampicillin and metronidazole as standard materials. The effectiveness of some compounds was measured as oxidants, and the results showed that compounds T1 and T6 gave medium-strength effectiveness, while compounds T4 and T5 gave weak effectiveness compared to ascorbic acid as a standard material. The blind molecular docking of six compounds was studied for a group of receptors (for bacteria) (7sie) as well as (4h2j) and (7v67) for fungi. The study showed the effective binding sites for each receptor with each compound separately. Furthermore, the study showed that the amino acids of the receptors associated with each compound, and also showed the type of binding between them, as well as the length of the distance of binding between amino acids and the compounds.

CONFLICT OF INTEREST

The authors declare that there is no conflict of interests regarding the publication of this

manuscript.

REFERENCES

1. Amin A, Qadir T, Sharma PK, Jeelani I, Abe H. A Review on The Medicinal And Industrial Applications of N-Containing Heterocycles. The Open Medicinal Chemistry Journal. 2022;16(1).
2. Uppadhayay RK, Kumar A, Teotia J, Singh A. Multifaceted Chemistry of Tetrazole. Synthesis, Uses, and Pharmaceutical Applications. Russ J Org Chem. 2022;58(12):1801-1811.
3. Frija LMT, Ismael A, Cristiano MLS. Photochemical transformations of tetrazole derivatives: applications in organic synthesis. Molecules (Basel, Switzerland). 2010;15(5):3757-3774.
4. da Silva L, Sánchez M, Ibarra-Rodriguez M, Freeman HS. Isomeric tetrazole-based organic dyes for dye-sensitized solar cells: Structure-property relationships. J Mol Struct. 2022;1250:131749.
5. Dhiman N, Kaur K, Jaitak V. Tetrazoles as anticancer agents: A review on synthetic strategies, mechanism of action and SAR studies. Bioorganic & Medicinal Chemistry. 2020;28(15):115599.
6. Jaiswal S, Verma K, Dwivedi J, Sharma S. Tetrazole derivatives in the management of neurological disorders: Recent advances on synthesis and pharmacological aspects. Eur J Med Chem. 2024;271:116388.
7. Swami S, Sahu SN, Shrivastava R. Nanomaterial catalyzed green synthesis of tetrazoles and its derivatives: a review on recent advancements. RSC advances. 2021;11(62):39058-39086.
8. Kaushik N, Kumar N, Kumar A, Singh UK. Tetrazoles: Synthesis and Biological Activity. Immunology, Endocrine & Metabolic Agents in Medicinal Chemistry. 2018;18(1):3-21.
9. Myznikov LV, Vorona SV, Zevatskii YE. Biologically active compounds and drugs in the tetrazole series. Chemistry of Heterocyclic Compounds. 2021;57(3):224-233.
10. Taylor RD, MacCoss M, Lawson ADG. Rings in Drugs. J Med Chem. 2014;57(14):5845-5859.
11. Verma A, Kaur B, Venugopal S, Wadhwa P, Sahu S, Kaur P, et al. Tetrazole: A privileged scaffold for the discovery of anticancer agents. Chemical Biology & Drug Design. 2022;100(3):419-442.
12. Gao F, Xiao J, Huang G. Current scenario of tetrazole hybrids for antibacterial activity. Eur J Med Chem. 2019;184:111744.
13. Kong Q, Yang Y. Recent advances in antibacterial agents. Bioorganic and Medicinal Chemistry Letters. 2021;35:127799.
14. Gujja V, Sadineni K, Epuru MR, Rao Allaka T, Banothu V, Gunda SK, Koppula SK. Synthesis and in Silico Studies of Some New 1,2,3-Triazolyltetrazole Bearing Indazole Derivatives as Potent Antimicrobial Agents. Chemistry & Biodiversity. 2023;20(12).
15. Patel HC, Patel MS, Parekh JN, Chudasama DD, Dalwadi P, Kunjadiya A, et al. In silico and in vitro evaluation of newly synthesized pyrazolo-pyridine fused tetrazolo-pyrimidines derivatives as potential anticancer and antimicrobial agents. Journal of Biomolecular Structure and Dynamics. 2023:1-24.
16. Kabi AK, Sravani S, Gujjarappa R, Garg A, Vodnala N, Tyagi U, et al. An Overview on Biological Evaluation of Tetrazole Derivatives. Materials Horizons: From Nature to Nanomaterials: Springer Singapore; 2022. p. 307-349.
17. Zhang N, Ma S. Recent development of membrane-active molecules as antibacterial agents. Eur J Med Chem. 2019;184:111743.
18. Zhang S, Liu Y, Javeed A, Jian C, Sun J, Wu S, Han B. Treatment of allergy: Overview of synthetic anti-allergy small molecules in medicinal chemistry. Eur J Med Chem. 2023;249:115151.
19. Labib MB, Fayez AM, El-Nahass ELS, Awadallah M, Halim PA. Novel tetrazole-based selective COX-2 inhibitors: Design, synthesis, anti-inflammatory activity, evaluation of PGE2, TNF-α, IL-6 and histopathological study. Bioorg Chem. 2020;104:104308.
20. DiPuma T, Thabthimthong T, Kelley EH, Konczak K, Beulke M, Herbert C, et al. Tetrazole-based inhibitors of the bacterial enzyme N-succinyl-l,l-2,6-diaminopimelic acid desuccinylase as potential antibiotics. Bioorganic & Medicinal Chemistry Letters. 2023;83:129177.
21. Mikolaichuk OV, Zarubaev VV, Muryleva AA, Esaulkova YL, Spasibenko DV, Batyrenko AA, et al. Synthesis, structure, and antiviral properties of novel 2-adamantyl-5-aryl-2H-tetrazoles. Chemistry of heterocyclic compounds. 2021;57(4):442-447.
22. Valentini A, Schultz-Knudsen K, Højgaard Hansen A, Tsakoumagkou A, Jenkins L, Christensen HB, et al. Discovery of Potent Tetrazole Free Fatty Acid Receptor 2 Antagonists. J Med Chem. 2023;66(9):6105-6121.
23. Neochoritis CG, Zhao T, Dömling A. Tetrazoles via Multicomponent Reactions. Chem Rev. 2019;119(3):1970-2042.
24. Bredael K, Geurs S, Clarisse D, De Bosscher K, D'hooghe M. Carboxylic Acid Bioisosteres in Medicinal Chemistry: Synthesis and Properties. Journal of Chemistry. 2022;2022:1-21.
25. Kf H, Hh E. Synthesis, Characterization, Biological Evaluation and Anti Corrosion Activity of Some Heterocyclic Compounds Oxazepine Derivatives from Schiff Bases. Organic Chemistry: Current Research. 2013;2(3).
26. F. Ghazi YA, Mahdi M, Dawood A. Theoretical Drug Design, Molecular Docking And ADME Study Of New 1,3,4-Oxadiazole Derivatives: Promising Anticancer Agents Against Both Breast And Lung Cancers. Egyptian Journal of Chemistry. 2021;0(0):0-0.
27. Dopico AM. Natural Bile Acids and Synthetic Analogues Modulate Large Conductance Ca^{2+}-activated K^{+} (BKCa) Channel Activity in Smooth Muscle Cells. The Journal of General Physiology. 2002;119(3):251-273.
28. Crystallography: Protein Data Bank. Nature New Biology. 1971;233(42):223-223.
29. Valdés-Tresanco MS, Valdés-Tresanco ME, Valiente PA, Moreno E. AMDock: a versatile graphical tool for assisting molecular docking with Autodock Vina and Autodock4. Biol Direct. 2020;15(1):12-12.
30. Kondapuram SK, Sarvagalla S, Coumar MS. Docking-Based Virtual Screening Using PyRx Tool: Autophagy Target Vps34 as a Case Study. Molecular Docking for Computer-Aided Drug Design: Elsevier; 2021. p. 463-477.
31. Enisoglu Atalay V, Asar S. Determination of the inhibition effect of hesperetin and its derivatives on Candida glabrata by molecular docking method. The European Chemistry and Biotechnology Journal. 2024(1):27-38.